Analytical Methods

Accepted Manuscript

This article can be cited before page numbers have been issued, to do this please use: G. Marucci, A. Beeby, A. W. Parker and C. E. Nicholson, *Anal. Methods*, 2018, DOI: 10.1039/C8AY00016F.

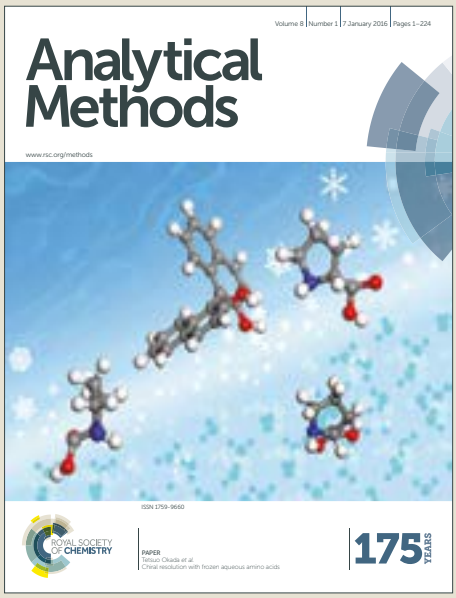

ROYAL SOCIETY OF CHEMISTRY

rsc.li/methods

View Article Online
DOI: 10.1039/C8AY00016F

Journal Name

ARTICLE

Raman spectroscopic library of medieval pigments collected with five different wavelengths for investigation of illuminated manuscripts.

xReceived 00th January 20xx,
Accepted 00th January 20xx

DOI: 10.1039/x0xx00000x

www.rsc.org/

G. Marucci[a], A. Beeby [b] and A. W. Parker [c] and C.E. Nicholson *[a]

Raman spectroscopy is widely applied in the cultural heritage field to perform non-destructive measurements *in situ,* in order to identify materials, specifically pigments. The spectra collected can be challenging to interpret because certain source laser wavelengths may be absorbed by specific pigments, leading to large fluorescence backgrounds which obscure the weak Raman signals, or worse cause photodegradation of the sample. Furthermore, the reference spectra for a specific pigment obtained from a particular laser wavelength is not always availible and is a crucial step in the detective work of pigment identification, especially when the resonance Raman effect can enhance some signals. As the range of lasers available increases, spectral libraries do not always record spectra acquired with the same wavelength used to carry out the measurements in field. In this work, reference spectra of 31 different componds, mostly used in mediaeval manuscripts as pigments and inks, are recorded. Five different wavelengths were used as excitation sources. The aim is to provide a useful and more complete reference source to enable better planning of which laser wavelength is the most appropriate to study a specific set of pigments, and to allow comparisons between spectra acquired with the same wavelength, leading to the unequivocal pigment identification in a step by step manner.

Introduction

The use of analytical techniques for the study of objects of historical and artistic interest has increased in the last thirty years, providing useful information about artists' techniques, the provenance of materials, the nature of degradation processes [1], authentication and dating. The priceless nature of works of art has driven scientists to employ non-invasive and non-destructive techniques. This, coupled with the high insurance values of the articles, essentially prevents the analysis of objects in host laboratories: work has to be done within the conservation studios of the host institution. Over the past decade, this has been achieved with the advent of portable, instrumentation that can be taken to the host libraries or institutions for in situ investigations on the fly. Among the different techniques that are routinely employed for the analysis of artefacts or manuscripts, micro-Raman spectroscopy has proven to be an extremely powerful, due to its portability, specificity, spatial resolution and non-contact, non-destructive nature [2-31]. The first effective application of Raman spectroscopy on cultural heritage objects was on illuminated manuscripts to identify pigments [32], and it has since been used to study a wide variety of materials including paper [33], binder media [34], inks [35, 36], glass [5, 9, 10, 18], ceramics and pottery [7, 8], gemstones [20], stones and rocks from archaeological sites [19, 30], degradation products [3]. The availability of a spectral library is therefore essential to help identify the materials deployed [34, 37-39]. A few portable Raman spectrometers are now commercially available, but these should be used with extreme caution: in many examples, the power of the laser light source is much higher than we would advocate and may cause damage to the artefact. Furthermore, commercially available portable instruments usually have a single laser source, in rare cases two, which are not necessarily the best ones to investigate the wide variety of pigments that can be found on the same artefact, positive identifications can often be difficult [26, 31]. Indeed, pigments respond differently to laser irradiation according to their nature (dyes or pigments, colour, etc.). In certain cases, for example, where the laser wavelength matches or is close to the absorption bands of the pigment being analysed, the Resonance Raman effect can lead to excellent sensitivity, but, in some cases, some absorption can also lead to large interfering, luminescent background signals which hide the low intensity Raman signals. The selection of the most appropriate wavelength for the identification of pigments then is of great interest and importance.

Portable equipment means compromises have to be made in comparison with fixed laboratory equipment. Portable systems tend to sacrifice spectral resolution and sensitivity [31]. This work provides an updated library of pigments' Raman spectra

a. Northumbria University, Applied Sciences, Newcastle upon Tyne, NE1 8ST
b. Durham University, Chemistry Department, DH1 3LE
c. STFC Rutherford Appleton Laboratory, Harwell Campus, Didcot, OX11 0QX
Electronic Supplementary Information (ESI) available: figures of pigments' spectra, from 1 to 30; the data of the Raman spectra collected at the different wavelengths. See DOI: 10.1039/x0xx00000x

View Article Online
DOI: 10.1039/C8AY00016F

acquired using different laser wavelengths in order to supply the best spectrum possible for each pigment for comparison to the data collected in situ. The pigments have been chosen as representative of those used in illuminated manuscripts between Vth- XVIth centuries in Europe [32, 36, 40-67].

Experimental

Instrumentation

Two different Raman spectrometers have been used, equipped with different lasers. The first was a Horiba Jobin Yvon LabRAM HR confocal Raman microscope, equipped with a Peltier-cooled CCD and 50× LWD Leica objective. The instrument has four different laser sources available, 488 nm, 532 nm, 632.8 nm and 785 nm providing a diffraction limited laser spot from 1 to 2 µm diameter. Each laser source has different maximum power values that can be reduced using neutral density filter (100% 50%, 25%, 10%, 1%, 0.1 % and 0.01%). Reported laser powers were measured after the objective lens in the sample plane. A 600 l/mm grating was used for measurements using the 532 nm, 632.8 nm and 785 nm laser, and an 1800 l/mm grating used for the 488 nm laser. The minimum wavenumber for each laser wavelength , dictated by the edge filters in the spectrometer were 200 cm^{-1}, 120 cm^{-1}, 70 cm^{-1}, 100 cm-1 respectively for the 488 nm, 532 nm, 632.8 nm and 785 nm lasers. All the acquisition operations were controlled by Lab Spec 6-Horiba Scientific software.

For excitation at 830 nm, a Renishaw InVIa micro-Raman spectrometer (Rutherford Appleton Laboratory, Harwell Campus, Didcot), with 830 nm laser source, a silicon CCD detector and Nikon L-PLAN SLWD 50x/0.45. The resulting laser spot was circa 2 µm in diameter. The spectral range recorded was 70-1800 cm^{-1}, with a 1200 l/mm grating. The maximum laser power was 55 mW, and this could be reduced to lower levels (50%, 25%, 10%, 5%, 1%, 0.5%, 0.1% and 0.05%). Again, the laser power was recorded after the objective in the sample plane.

A silicon standard sample was used as reference for calibration (520 cm^{-1}). The time of acquisitions and number of accumulations was decided on a sample-by-sample basis.

To be able to compare spectra acquired with different devices, spectra were corrected for the instrumental response by comparison to the spectra obtained for a broad-band source [68, 69]. A stable white light source (HL-2000-CAL Ocean Optics), whose spectral distribution was known (and can be approximated by a black body radiator of 2939 K), was used to generate a correction curve. The lamp emission spectrum was provided as photons/ ($\Delta\lambda$*t), where $\Delta\lambda$ is the bandwidth detected by the spectrometer, and t the time unit. It had to be multiplied by λ^2 (where λ is the emission wavelength), in order to obtain the spectrum in terms of photons/t*$\Delta\bar{\upsilon}$ of Raman shift. The calibration lamp spectrum was recorded for every wavelength laser using the same scan-conditions as used for the sample measurements and covering the same wavenumber range. Using this correction curve, all of the Raman spectra were corrected for instrument response. No background subtraction was performed, since one of the goals of this work was to provide a library that helps to decide which the best wavelength to investigate a certain pigment is, so any luminescent background that may detract from the signal or prove diagnostic was recorded. All the spectra have been normalized to a maximum intensity of 1 in the graphs (Fig.1-Fig.30) available in the electronic supplementary information (ESI). In the ESI, the raw ASCII data of the spectra can be found. corrected for the instrument response. Thus, relative intensities of peaks may be obtained and compared directly.

Classification of the spectra

A classification of the quality of the spectra collected (Table 1) was made, in order to establish the optimum wavelength for investigating the presence of a specific pigment, and which wavelength provides the maximum number of positive identifications. To classify them, a criterion to value the quality of the spectrum had to be established and the signal to noise ratio was considered appropriate. Even though this parameter is meaningful if applied to a single peak or band it does not give an evaluation of the whole spectrum, since to identify a Raman spectrum a "finger printing" approach is often used; analysing the most intense peak and then the following less intense ones to confirm or refute the identification. In this study only the signal to noise ratio of highest peak of every spectrum was used to evaluate the whole spectrum. However, spectra showing only one peak were not included because a single peak is insufficient to unequivocally identify a pigment [70]. In spectroscopy, the signal to noise ratio, SNR, is defined as

$$SNR = \frac{I}{\sigma}$$

Where I is the average intensity of the signal and σ is its standard deviation [71]. However, the noise is the result of different sources. So that

$$\sigma = \sqrt{(\sigma_s^2+\sigma_b^2+\sigma_d^2+\sigma_r^2)}$$

where σ_s is the uncertainty of the measurements known as signal shot noise. σ_b is the noise due to the background, that includes fluorescence of the sample and stray light. σ_d is the noise generated by the dark current of the detector and the σ_r is the readout noise caused by the conversion from the electronic signal to a digital value in the CCD camera (and subsequent transfer from the detector to the computer) [71]. The signal shot noise is the square root of the signal intensity according to the Poisson statistic, since the emission and detection of photons are random event [72, 73]. However, background and the dark noise are detected in the same way as the Raman signal and similarly they are equal to the square root of the background intensity and dark current [71] respectively. Finally, the read out noise is the standard deviation of the numerical value the electrons from the detector device are converted into when digitized [71]. Thus, the overall signal to noise ratio is defined as

View Article Online
DOI: 10.1039/C8AY00016F

$$SNR = \frac{I}{\sqrt{(\sigma_s^2 + \sigma_b^2 + \sigma_d^2 + \sigma_r^2)}}$$

To calculate the signal to noise ratio, the contribution of the dark noise and the read out noise were considered negligible, which is appropriate for the scientific grade CCD camera employed in the spectrometers, while the background noise was the result of the square root of the difference of intensities between the spectra before and after background correction. A peak may be defined as at least 2 or 3 times the intensity of the noise [70, 72]. So that the spectra were classified as "very good" spectrum (++) when the SNR > 100; "good spectrum" when 3 < SNR < 100; "spectrum not identifiable" when SNR < 3 and/or the spectrum presented only one peak; "bad spectrum" when no spectrum at all was recorded.

Pigment	488 nm	532 nm	632.8 nm	785 nm	830 nm
Minium	+	+	++	++	++
Haematite	±	+	+	+	++
Red Ochre	+	+	+	+	+
Caput Mortum	+	+	+	++	++
Vermillion	+	+	++	++	++
Cinnabar	+	+	++	++	++
Realgar	-	±	++	++	++
Kermes	-	-	-	-	-
Cochineal	±	+	-	+	-
Orcein	+	+	+	+	+
Brazil Wood	-	-	-	-	-
Purple Madder	+	+	+	+	+
Alizarin Crimson	+	±	+	+	+
Alizarin Purple	+	-	-	+	+
Raw Umber	±	+	±	-	+
Sepia	-	+	+	+	+
Indigo	±	+	+	+	++
Azurite	+	+	+	+	+
Ultramarine	+	++	+	+	+
Orpiment	+	++	++	++	++
Lead Tin Yellow I	++	++	++	++	++
Yellow Ochre	+	+	+	+	++
Massicot	++	++	++	++	++
Gamboge	+	±	-	+	+
White Lead	+	+	++	++	++
Verdigris	+	+	+	±	+
Malachite	+	+	+	-	+
Carbon Black	+	+	+	±	+
Ivory Black	+	+	+	+	+
Lamp Black	+	+	+	+	+
Iron Gall	-	+	-	±	±
Bistre	+	±	+	+	+

Table 1 Classification of the spectra. ++ very good spectrum; += good spectrum; ±= spectrum with peaks but pigment not identifiable; -= no spectrum

Materials

Pigments and inks investigated were both pigments and dyes, chosen in accordance with the literature, most commonly used in manuscripts between Vth-XVth centuries, supplied by L. Cornelissen & Son (London) and Kremer Pigmente GmbH & Co. KG (Aichstetten, Germany). Iron gall ink, Brazil wood and kermes were made following ancient recipes[74]. Analysis of pure pigments using the 532nm and 632.8 nm lasers was made by sampling through the wall of a glass vial containing the pigments. Indeed, the use of a confocal microscope allows collecting radiation coming only from the focal plane, so that there is no signal related to the glass [72]. However, using the 785nm excitation source the spectra presented a large background at around 1400 cm^{-1} [75] so pellets of pigments were prepared to obtain Raman spectra without glass contribution. The measurements performed with 488 nm and 830nm excitation were also run on pellets. They were prepared by pressing a mixture of the pigment and a 10 % w/w of a wax binder, (BM-0002-1CEREOX® Licowax C Micropowder). To ensure the homogeneity of the samples the mixture of wax and pigment was shaken for 3 minutes with a frequency of 25 s^{-1}, and pellets were then formed using a hydraulic press, with 9 tonnes/surface pressure. The spectra collected do not show any signals attributable to the wax.

Results and discussion

A total of 31 pigments have been analysed using 5 different incident wavelength laser sources. The spectra are represented in Fig.1-Fig.30 (in the ESI). They are ordered by observed colour (red, purple, blue, yellow, white, green, black and inks). In Table 1 the positive identifications are summarized. Table 2 to 6 list the wavenumber of the main peaks detected, with references from previous works [37-39, 76-81], where spectra have been reported for similar conditions. Each table refers to a single wavelength laser source. The first column provides the highest observed peak in the measured spectral range for that wavelength. In the second column the other peaks, in decreasing order of intensity, can be found; in the other columns the name and the compounds of the pigment. In the last column, the values of power density are recorded.

View Article Online
DOI: 10.1039/C8AY00016F

To use the library:

1) Select the table pertinent to the laser wavelength used to carry out the measurements;
2) Look for the highest intensity peak in the first column;
3) Check the other peaks in the second column. The third column provides the name of the pigment.

λ_0=488 nm	Spectral Range (200-2500 cm^{-1})			
Main Band cm^{-1}		Pigment Name		Power density $mW/\mu m^2$
200	458, 291, 524, 276, 550sh, 379, 305, 616, 595	Lead Tin Yellow I	Tin (II) sulfide, Lead (II) stannate, Pb_2SnO_4	3.90
225	291, 409	Caput Mortuum	Iron (III) Oxide, Fe_2O_3	0.39
255	346	Cinnabar	Mercury (II) sulfide, HgS	0.39
255	346, 288sh	Vermillion	synthetic mercury (II) sulfide, HgS	0.39
280br	391	Haematite	Iron (III) Oxide, Fe_2O_3	1.02
289	386, 424,	Massicot	Lead (II) Oxide, PbO	3.90
324	951, 233, 942sh, 1440, 1419, 216sh, 255, 1360, 688, 1668, 1055	Verdigris	Copper (II) acetate,$Cu(CH_3COO)_2$ $[Cu(OH)_2]_3$ $2H_2O$	3.90
354	311, 294, 382, 203,	Orpiment	Arsenic (III) Sulfide, As_2S_3	3.90
402	466, 1575, 1429, 1420, 1095, 249, 765, 838[39], 938, 1460, 1495, 541, 281, 267	Azurite	Basic Copper (II) Carbonate, $Cu_3(CO_3)_2$ $(OH)_2$)	1.99
459	1497br, 1617br	Raw Umber	Iron (III) Oxide, Fe_2O_3 +Manganese (IV) Oxide, MnO_2	3.90
461	283br, 695br	Red Ochre	Iron (III) Oxide, Fe_3O_4 +clay +silica	3.90
549	584, 1096, 1648, 256, 806, 2191, 1363	Ultramarine	$Na_6Ca_6(Al_6SI_6O_{24})$ $(SO_4, S, S_2, S_3, Cl, OH)_2$	3.90
550	480,1094br, 390[37],233	Minium/ Red Lead	Lead (II, IV) Oxide, Pb_3O_4	0.39
1027	1008, 385, 1133, 491, 418sh, 297, 632.8, 547, 676, 241, 1084	Yellow Ochre	Iron (III) Oxide Hydrate, Fe_2O_3 H_2O +clay +silica	3.90
1052	1056sh, 1365br, 1297, 693, 422br, 1134	White Lead	Basic Lead (II) Carbonate , $2PbCO_3$ $Pb(OH)_2$	0.39
1306	1479[82], 1702[82], 1255	Cochineal	Carminic acid, $C_{22}H_{20}O_{13}$	0.08
1321[82]	1478, 1280sh, 1161[82]	Purple Madder	Alizarin $C_{14}H_8O_4$ and Purpurin $C_{14}H_8O_5$	3.99
1322[82]	1476[82], 1297sh, 1271	Alizarin Purple	Alizarin $C_{14}H_8O_4$	3.90
1477[82]	1325[82], 1290[82], 1163, 906, 839, 660[82], 480	Alizarin Crimson	Alizarin $C_{14}H_8O_4$	3.90
1495	434, 225, 272, 536, 1062, 1103, 1367, 356, 1297, 721, 755	Malachite	Basic Copper (II) carbonate, Cu_2CO_3 $(OH)_2$	3.90
1573br	1347br	Lamp Black	Carbon, C	3.90
1581br	1361 br	Carbon Black	Carbon, C	3.90
1585	1703, 1363, 1252	Indigo	Indigo, $C_{16}H_{10}N_2O_2$	3.90
1592br		Bistre	Wood soot, Carbon C	1.99
1594br	1362br, 469br	Ivory Black	Calcium hydroxide phosphate, $Ca_5(OH)$ $(PO_4)_3$ + Carbon, C	3.90
1594	1632	Gamboge	Gambogic Acid, $C_{38}H_{44}O_8$	3.90
1642	1608, 1505br, 1278,1192br, 489	Orcein	Natural Red 28, $C_{28}H_{24}N_2O_7$	3.90

Table 2 Characteristic peaks of Raman spectra of pigments acquired with a 488 nm excitation source. Broad bands are labelled with "br", shoulder bands are labelled with "sh".

Red Pigments. For convenience, the pigments can be divided into two major groups. The first is the iron oxide compounds (haematite, red ochre and caput mortuum, which belongs also to the inks group as well), and the others (cinnabar, vermillion, minium/red lead). All the iron oxide (Figure 2 – Figure 4) compounds show the main peaks at around 223 cm^{-1}, between 290 cm^{-1}, around 407 cm^{-1}, but only the spectra acquired with 532nm and the 632.8 nm excitation beams show an intense peak between 1316 cm^{-1} and 1323 cm^{-1}. The intensity enhancement is attributed to resonance effects since the

View Article Online
DOI: 10.1039/C8AY00016F

λ_0=532nm	Spectral Range (100-2500 cm^{-1})			
Main Band cm^{-1}		Pigment Name		Power density $mW/\mu m^2$
130[83]	96[83], 458, 293, 275, 252, 379[77], 304, 615[77]	Lead Tin Yellow I	Tin (II) sulfide, Lead (II) stannate, Pb_2SnO_4	2.06
143[77]	290, 386, 425, 169sh	Massicot	Lead (II) Oxide, PbO	0.82
178[76, 77, 84]	151[76, 77], 169[76, 84], 430[77], 220[77], 266[76, 84], 1491[76, 84], 203sh, 532[76, 77], 535sh[76, 77, 84], 350sh[76, 77], 509[77], 1092[76, 84], 1060[76, 77], 720[76, 84], 1459[77], 751[77, 84], 593	Malachite	Basic Copper (II) carbonate, $Cu_2CO_3(OH)_2$	2.06
254	290, 342	Cinnabar	Mercury (II) sulfide, HgS	0.08
254[77]	343[77], 290	Vermillion	synthetic mercury (II) sulfide, HgS	0.08
268	214, 582br,	Raw Umber	Iron (III) Oxide, Fe_2O_3 +Manganese (IV) Oxide, MnO_2	8.21
324	949[76, 84], 127[76, 84], 1439[76, 84], 297, 183[77], 234[76], 703[76, 77], 1296, 254[84], 1061[76], 1133, 1641br	Verdigris	Copper (II) acetate,$Cu(CH_3COO)_2[Cu(OH)_2]_3\ 2H_2O$	2.06
354[83]	311, 293, 382, 154, 203[83], 136[83], 180[83], 234, 490 br, 589br,	Orpiment	Arsenic (III) Sulfide, As_2S_3	0.82
356[83]	343[77], 338, 192[83], 183[77], 221	Realgar	Arsenic (III) Sulfide, As_4S_4	0.01
400[77]	247[77], 1096[77], 1578[77], 1430[77], 1417, 132, 171, 281[77], 178, 138[77], 266, 154, 839, 764[77], 542, 737[77], 336	Azurite	Basic Copper (II) Carbonate, $Cu_3(CO_3)_2(OH)_2$)	2.06
547	1089br, 479, 474, 389,313, 227, 163 (a)	Minium/ Red Lead	Lead (II, IV) Oxide, Pb_3O_4	0.82
548[77]	1097[77], 1647[77], 2191[77], 1644[77], 257[77], 864, 275, 1369, 1905[77]	Ultramarine	$Na_6Ca_6(Al_6SI_6O_{24})$ (SO_4, S, S_2, S_3, Cl, OH)$_2$	2.06
1007	388, 416, 299[77], 1138, 245[83], 549, 495, 675,	Yellow Ochre	Iron (III) Oxide Hydrate, $Fe_2O_3\ H_2O$ +clay +silica	2.06
1050[77]	131, 1370br[77], 151sh, 418sh, 1635	White Lead	Basic Lead (II) Carbonate , 2Pb CO_3 Pb(OH)2	0.82
1316	291, 227, 409, 613, 497, 247	Caput Mortuum	Iron (III) Oxide, Fe_2O_3	0.82
1321	1479, 1159[77]	Purple Madder	Alizarin $C_{14}H_8O_4$ and Purpurin $C_{14}H_8O_5$	0.82
1322	(b)	Cochineal	Carminic acid, $C_{22}H_{20}O_{13}$	0.82
1322	1478	Alizarin Purple	Alizarin $C_{14}H_8O_4$	0.08
1323	290, 223, 407, 600, 238	Haematite	Iron (III) Oxide, Fe_2O_3	0.82
1351	460, 299, 674, 629, 230, 414	Red Ochre	Iron (III) Oxide, Fe_2O_3+clay +silica	0.82
1480[77]	1326	Alizarin Crimson	Alizarin $C_{14}H_8O_4$	0.08
1574br	1405br	Sepia	Melanin $C_{18}H_{10}N_2O_4$	0.82
1572	1335	Lamp Black	Carbon, C	8.21
1582	1361, 1701, 1251, 1628, 546, 598, 1461, 1485, 1312, 941, 756, 249, 1222	Indigo	Indigo, $C_{16}H_{10}N_2O_2$	8.21
1582	1346	Carbon Black	Carbon, C	8.21
1587	1351[77]	Ivory Black	Calcium hydroxide phosphate, $Ca_5(OH)(PO_4)_3$ + Carbon, C	8.21
1592br		Bistre	Wood soot	2.06
1600	1632.8	Gamboge	Gambogic Acid, $C_{38}H_{44}O_8$	2.06
1639	1499, 1335, 1275, 1191, 483	Orcein	Natural Red 28, $C_{28}H_{24}N_2O_7$	2.06
1644	1601, 1353, 560 (c)	Iron Gall Ink	Ferric Gallate $C_{21}H_{15}FeO_{15}$	0.96

Table 3 Characteristic peaks of Raman spectra of pigments acquired with a 532 nm excitation source (a) range between 100 and 2500 cm^{-1}, (b) range between 108 and 2500cm^{-1}, (c) range between 150-2500 cm^{-1}. Broad bands are labelled with "br", shoulder bands are labelled with "sh".

absorption edge for Fe_2O_3 is at 580 nm. Spectra acquired with 488 nm all have poor signals, because of absorption by the pigment. Unfortunately, the red ochre (Figure 3), which is a mixture of iron oxides, clays and silica, is the one that provided

View Article Online
DOI: 10.1039/C8AY00016F

lowest signal to noise ratio with all the laser sources compared to haematite and caput mortuum. The red ochre spectra are indeed affected by fluorescence, likely related to the presence of a heterogeneous matrix. In the second group, minium (Figure 1), or red lead, is a lead oxide, whose the main peak resulting from 632.8 nm excitation is at 121 cm^{-1}, due to the deformation of the O-Pb-O angle. This was not detectable with the other wavelengths because of the edge filters cutting off low wavenumbers or attenuating the signal, and in literature studies of manuscripts this band is often omitted for this reason. However, contrary to the report by Burgio et al. [1] who reported sample damage when using 488 nm and 514.5 radiations, it was possible to detect the pigment thanks to a low power density at 0.39mW/μm^2. Cinnabar and vermillion (Figure 5- Figure 6) are the mineral and synthetic forms of mercury sulphide, both show indeed the same very strong peak at 251-255 cm^{-1}. They are both detectable with all the five wavelengths, and only low laser power is required when working with 532 nm and 488 nm lasers to prevent saturation of the detector even at short acquisition times.

Purple Pigments. Cochineal (Figure 8), orcein (Figure 9), brazil wood, kermes, purple madder (Figure 10), alizarin crimson (Figure 11) and alizarin purple (Figure 12) are all organic compounds and, these spectra are prone to be affected by fluorescence depending on the wavelength of the excitation source. The spectrum collected with the 830 nm of cochineal does not show any Raman bands, as well as the 632.8 nm. Orcein, purple madder and alizarin crimson were detectable with all the wavelengths, while alizarin purple did not provide any spectrum with the 532 nm (absorption at 530 nm) and 632.8 nm radiation. For kermes and brazil wood, no spectra could be obtained at any of the five laser wavelengths.

Blue Pigments. Indigo (Figure 14) provides better spectra with the NIR and IR laser since it possesses a broad absorption band in the visible range [85]. However, it is still possible to recognise the pigment, thanks to the peak at 1580 cm^{-1} circa and 545 cm^{-1} also with lower wavelengths, which are superimposed upon the weak fluorescence from this material. Azurite (Figure 15) yields a good spectrum with all the wavelengths except the 632.8 nm laser source, attributed to the strong absorption by the pigment at ca. 600nm. When using the infrared sources at 785 and 830 nm, a very low energy (785 nm and 830 nm, 3.58 and 8.69 $mW/\mu m^2$) was used: at higher levels absorption of the radiation and localised heating of the sample results in its degradation. When the particles of azurite do not disperse the heat efficiently and the rate of heat inside the single grain is higher than the rate of heat outside, they thermo-degrade[86]. Ultramarine (Figure 16) can be identified by the strong band at 550 cm^{-1} using all excitation wavelengths. The absorption band at around 610 nm means that the 532 nm and 632 nm excitation sources, close to the electronic absorption wavelength, benefit from strong resonance enhancement and yield a progression of bands due to the bending of S_3^{-}[87]. Indeed, in the spectrum collected with the 488nm shows clearer a band at 584 cm^{-1} result of the S_2^- vibration, which with the other sources appears only as a shoulder of the main peak at 550 cm^{-1}.

Brown pigment. The only brown pigment investigated was raw umber (Figure 13). It is a mixture of iron oxides and manganese oxides. Investigation at 830 nm shows bands at 292 cm^{-1}, 610 cm^{-1}, 225 cm^{-1}, 390 cm^{-1} and 725 cm^{-1}. Excitation with the green laser presents weak bands at 268 cm^{-1}, 214 cm^{-1} and 582 cm^{-1}. No satisfactory Raman spectra were obtained with the other laser excitation wavelengths, 488, 632.8 nm, 785 or 830 nm.

Yellow Pigments. Orpiment (Figure 17) is easily detectable with all the excitation wavelengths, requires only low laser powers to detect, and it may indeed cause saturation of the detector under some conditions. The main chromophore of yellow ochre is limonite, an iron oxy-hydroxide, and this pigment shows the same main peaks of the mineral at all wavelengths. Ochres come in a range of compositions, due to natural variance of the mineral and the Raman spectrum (Figure 18) can therefore reflect these differences when collecting spectra from real historical artefacts. Lead tin yellow type I (Figure 19) and massicot (Figure 20) are both easily identified with the different laser wavelengths, but extra care has to be taken since they are both lead compounds and careful management of the laser power is required to avoid photo degradation: Burgio records alteration at 10 mW with 514.5 nm excitation source [1]. In the field, this simply requires using a reliable power meter prior to measurement to ensure one knows precisely the light power being delivered at the sample surface and to work well below the damage thresholds. Lead tin yellow (Figure 19) and massicot (Figure 20) were detected with the 488 nm source at 3.9 mW/ μm^2 and with the 532 nm at 2.06 mW/ μm^2 for lead tin yellow type I and 0.82 mW/μm^2 for massicot, without any degradation. No damage at the sample was noticed with the higher wavelengths and if low values of power (0.37mW/ μm^2 with 830nm laser) were used it was to avoid the detector saturation. The organic nature of gamboge (Figure 21) causes fluorescence in the spectra, especially with higher frequency sources. The 830 nm laser is the one that yields the best spectrum, with an intense peak at 1593 cm^{-1}.

White pigment. When suspecting the presence of white lead (Figure 22) it is necessary to employ low laser power (0.39 mW/μm^2 with 488nm and 0.12 mW/ μm^2 with 830 nm) because like other lead compounds it can easily be photodegraded by the laser [88, 89]. The highest intensity peak is observed at 104 cm^{-1} that requires a good laser light rejection cut off filter. As it can be seen from the spectra presented in Figure 22 this band is clearly observed in our system when using the 632.8 nm excitation, where the notch filter has a

View Article Online
DOI: 10.1039/C8AY00016F

shorter cut off. However, it remains observable using 830 nm excitation source, but lies on top of the sloping laser beam profile.

λ_0=632.8nm	Spectral Range (50-2500 cm-1)			
Main Band cm^{-1}		Pigment Name		Power density $mW/\mu m^2$
73,	1438, 950, 183, 232, 1300, 315, 1133, 1647, 1064(b)	Verdigris	Copper (II) acetate,Cu $(CH_3COO)_2$ $[Cu(OH)_2]_3$ $2H_2O$	1.16
104	70, 1050, 1365, 1475br, 412, 963, 677, 325(a)	White Lead	Basic Lead (II) Carbonate , $2Pb\,CO_3$ $Pb(OH)_2$	2.63
121[37, 38, 77]	549[37, 38, 77], 149[77], 390[37, 38, 77], 65, 223[37, 38, 77], 313[37, 38, 77], 480[37, 38], 84[38], 456sh, 290sh, 1094br[77](b)	Minium/ Red Lead	Lead (II, IV) Oxide, Pb_3O_4	2.63
127[77]	77, 193[77], 456[77], 273[77], 290[77], 524[77], 377[77], 336br	Lead Tin Yellow I	Tin (II) sulfide, Lead (II) stannate, Pb_2SnO_4	1.30
142[37, 38, 77]	288[37, 38, 77], 86[38], 70[38], 384[37, 38, 77], 215br, 423[38]	Massicot	Lead (II) Oxide, PbO	2.63
162	188, 89, 129, 226, 127, 439, 278, 359, 1501, 506, 1377	Malachite	Basic Copper (II) carbonate, Cu_2CO_3 $(OH)_2$	2.63
251[37, 77]	342[37, 77], 280sh[37, 77], 86, 104sh	Vermillion	synthetic mercury (II) sulfide, HgS	2.63
253	343, 283, 85, 102	Cinnabar	Mercury (II) sulfide, HgS	2.63
291[78]	1316, 226[78], 408[78], 610[78], 822br, 658br, 243sh	Caput Mortuum	Iron (III) Oxide, Fe_2O_3	2.63
293[39]	1320, 409[39], 609[38, 39], 224[39], 1086br, 660, 243[38, 39], 495[38, 39], 820br	Haematite	Iron (III) Oxide, Fe_2O_3	0.26
354[37, 77]	309[37, 77], 291[37], 153[37, 77], 381[37], 201[37], 66, 180[37], 104	Orpiment	Arsenic (III) Sulfide, As_2S_3	1.30
354[37]	185[77], 191[37], 221[37, 77], 230sh, 368sh[37], 58, 168sh, 143[37, 77], 120	Realgar	Arsenic (III) Sulfide, As_4S_4	1.30
408	292[37], 224, 657br, 610br	Red Ochre	Iron (III) Oxide, Fe_3O_4 +clay +silica	0.64
545[77]	1096[77], 86, 1370, 1662, 255, 286sh[77]	Ultramarine	$Na_6Ca_6(Al_6SI_6O_{24})$ $(SO_4, S, S_2, S_3, Cl, OH)_2$	2.63
657 br[78],		Raw Umber	Iron (III) Oxide, Fe_2O_3 +Manganese (IV) Oxide, MnO_2	0.26
1005[37]	385[37, 38], 1134, 1084, 670, 617, 547, 488[38], 296[37], 241, 92[38]	Yellow Ochre	Iron (III) Oxide Hydrate, Fe_2O_3 H_2O +clay +silica	2.63
1095[38]	835, 396, 761[38], 476br, 79, 240[38], 133, 171	Azurite	Basic Copper (II) Carbonate, $Cu_3(CO_3)_2$ $(OH)_2$)	2.63
1324[81]	1293, 1475, 1448[81], 1157[81], 825[81]	Purple Madder	Alizarin $C_{14}H_8O_4$and Purpurin $C_{14}H_8O_5$	2.63
1324	1594br	Carbon Black	Carbon, C	4.68
1333[77]	1585	Lamp Black	Carbon, C	2.63
1477	1325[81], 1291, 1187[81], 1160[81], 898[81], 837	Alizarin Crimson	Alizarin $C_{14}H_8O_4$	0.26
1573br		Iron Ink Gall	Ferric Gallate $C_{21}H_{15}FeO_{15}$	2.63
1578	1253, 1223, 756, 672, 596, 545, 309, 250, 274	Indigo	Indigo, $C_{16}H_{10}N_2O_2$	2.63
1585	1373br	Bistre	Wood soot, Carbon C	0.64
1592br	1392br	Sepia	Melanin $C_{18}H_{10}N_2O_4$	0.33
1597	1349[77]	Ivory Black	Calcium hydroxide phosphate, $Ca_5(OH)$ $(PO_4)_3$ + Carbon, C	2.63
1644	1518, 1408, 1277, 1189, 629, 595, 821, 525, 479,	Orcein	Natural Red 28, $C_{28}H_{24}N_2O_7$	2.63

Table 4 Characteristic peaks of Raman spectra of pigments acquired with a 632.8 nm excitation source. (a) range between 80 and 2500 cm^{-1}, (b) range between 50 and 2500 cm^{-1}. Broad bands are labelled with "br", shoulder bands are labelled with "sh".

Green Pigments. Verdigris (Figure 23) and malachite (Figure 24) both result in good Raman spectra for the shorter wavelengths and do not provide a spectrum with the 785 nm laser because of strong absorption of the light in this region [84]. However, the spectra obtained with the 830nm do present peaks at 150 cm^{-1}, 179 cm^{-1}, 218 cm^{-1}, 269 $cm^{-1}$to identify the pigments unambiguously.

View Article Online
DOI: 10.1039/C8AY00016F

λ_0=785nm	Spectral Range (100-2500 cm^{-1})			
Main Band cm^{-1}		Pigment Name		Power density W/ μm^2
549[77]	391, 314[77], 224[77], 234sh, 456, 480(a)	Minium/ Red Lead	Lead (II, IV) Oxide, Pb_3O_4	3.58
107	1051[77], 1055sh, 410, 320br, 679[77], 1136, 1441, 1640	White Lead	Basic Lead (II) Carbonate , 2Pb CO_3 $Pb(OH)_2$	3.58
129[77]	196[77], 457[77], 291[77], 274, 111, 524[77], 379[77], 337, 508, 304, 337, 432sh,	Lead Tin Yellow I	Tin (II) sulfide, Lead (II) stannate, Pb_2SnO_4	3.58
142[77]	288[77], 384[77], 214, 427	Massicot	Lead (II) Oxide, PbO	3.58
223[77]	290[77], 406[77]	Red Ochre	Iron (III) Oxide, Fe_3O_4 +clay +silica	3.58
253	343, 286, 107, 143	Vermillion	synthetic mercury (II) sulfide, HgS	0.96
254	343, 287, 108, 143, 201	Cinnabar	Mercury (II) sulfide, HgS	0.32
290	408, 224, 244, 609, 498, 1323br	Haematite	Iron (III) Oxide, Fe_2O_3	3.58
290	224, 407, 609, 244, 495, 1316	Caput Mortuum	Iron (III) Oxide, Fe_2O_3	3.58
353[77]	292, 202[77], 383, 325, 218, 472, 585, 653, 706	Orpiment	Arsenic (III) Sulfide, As_2S_3	3.58
354[77]	192[77], 181, 220, 343[77], 142[77], 165, 171[77], 368, 374, 328, 212	Realgar	Arsenic (III) Sulfide, As_4S_4	0.96
397	246, 464, 128, 1095, 1428, 762, 834, 1574,	Azurite	Basic Copper (II) Carbonate, $Cu_3(CO_3)_2$ $(OH)_2$)	3.58
482	1274, 1188[90], 592[90], 524[90], 809, 1463, 1492 , 1640[90]	Orcein	Natural Red 28, $C_{28}H_{24}N_2O_7$	3.58
550[77]	584sh[77], 256	Ultramarine	$Na_6Ca_6(Al_6SI_6O_{24})$ (SO_4, S, S_2, S_3, Cl, OH)	3.58
980	1430, 1338, 573 br	Iron Gall Ink	Ferric Gallate $C_{21}H_{15}FeO_{15}$	4.94
1007	1255, 1224, 384, 431, 1138, 495, 1410, 671	Yellow Ochre	Iron (III) Oxide Hydrate, Fe_2O_3 H_2O +clay +silica	3.58
1248br	1560br	Bistre	Wood soot, Carbon C	4.94
1293	1318[90], 1442,	Purple Madder	Alizarin $C_{14}H_8O_4$and Purpurin $C_{14}H_8O_5$	3.58
1303[90]	1321[77], 1473	Cochineal	Carminic acid, $C_{22}H_{20}O_{13}$	3.58
1350br	1550br	Sepia	Melanin $C_{18}H_{10}N_2O_4$	3.58
1430,	1136, 227	Verdigris	Copper (II) acetate,Cu $(CH_3COO)_2$ $[Cu(OH)_2]_3$ $2H_2O$	3.58
1431	1584, 1304	Lamp Black	Carbon, C	3.58
1474	1302, 1323[90]	Alizarin Purple	Alizarin $C_{14}H_8O_4$	3.58
1480[90]	1328, 1292[77], 480, 1192, 1462sh, 1451sh[90], 841, 1163[77, 90], 659, 904[77 90]	Alizarin Crimson	Alizarin $C_{14}H_8O_4$	3.58
1571	1580 sh, 250, 545[77], 597[77], 262, 674[77], 273, 756[77], 1223, 1308, 1459, 1362, 1015[77]	Indigo	Indigo, $C_{16}H_{10}N_2O_2$	3.58
1576	1332	Carbon Black	Carbon, C	3.58
1585[77]	1329	Ivory Black	Calcium hydroxide phosphate, $Ca_5(OH)$ $(PO_4)_3$ + Carbon, C	3.58
1592[77]	1297, 1620sh, 1136, 1062	Gamboge	Gambogic Acid, $C_{38}H_{44}O_8$	3.58

Table 5 Characteristic peaks of Raman spectra of pigments acquired with a 785 nm excitation source . (a) range between 200-2500 cm^{-1}**.** Broad bands are labelled with "br", shoulder bands are labelled with "sh".

View Article Online
DOI: 10.1039/C8AY00016F

λ_0=830nm	Spectral Range (100-2500 cm^{-1})			
Main Band cm^{-1}		Pigment Name	Compound	Power density mW/ μm^2
92	315, 949,179, 1296, 1436br	Verdigris	Copper (II) acetate,Cu $(CH_3COO)_2$ $[Cu(OH)_2]_3$ $2H_2O$	0.86
105	74, 1049, 1053, 416br, 679,	White Lead	Basic Lead (II) Carbonate , $2Pb\,CO_3$ $Pb(OH)_2$	0.12
120	549, 390, 151, 314, 142sh, 230br, 63, 85, 454	Minium/ Red Lead	Lead (II, IV) Oxide, Pb_3O_4	0.86
128^{79}	79, 196^{79}, 457^{79}, 292^{79}, 273^{79}, 112, 524^{79}, 379^{79}, 96, 304^{79}, 339, 432,	Lead Tin Yellow	Tin (II) sulfide, Lead (II) stannate, Pb_2SnO_4	0.37
142	87, 289, 70, 384, 217	Massicot	Lead (II) Oxide, PbO	0.37
150	179, 77, 218, 269, 430, 1061br, 1495	Malachite	Basic Copper (II) carbonate, Cu_2CO_3 $(OH)_2$	0.86
254^{79}	343^{79}, 283^{79}, 103, 85, 142	Vermillion	synthetic mercury (II) sulfide, HgS	0.12
254^{79}	343^{79}, 283^{79}, 103^{79}, 85^{79}	Cinnabar	Mercury (II) sulfide, HgS	0.12
287	222, 406, 605, 489, 241sh	Caput Mortuum	Iron (III) Oxide, Fe_2O_3	2.85
291	225, 408, 612, 244, 498, 1321br	Haematite	Iron (III) Oxide, Fe_2O_3	2.85
292	610br, 225, 390br, 725	Raw Umber	Iron (III) Oxide, Fe_2O_3 +Manganese (IV) Oxide, MnO_2	1.24
293	405, 398, 221, 608	Red Ochre	Iron (III) Oxide, Fe_3O_4 +clay +silica	2.85
353	191, 182, 220, 342, 166, 171, 142, 367374, 328, 123	Realgar	Arsenic (II) Sulfide, As_4S_4	0.37
354	311, 293, 154, 202, 136, 382, 369sh, 179, 105, 69	Orpiment	Arsenic (III) Sulfide, As_2S_3	0.12
401	248, 1093, 171 (a)	Azurite	Basic Copper (II) Carbonate, $Cu_3(CO_3)_2$ $(OH)_2$)	0.86
488	1275, 1192, 600br, 1333br,887, 1080, 432, 528	Orcein	Natural Red 28, $C_{28}H_{24}N_2O_7$	1.24
541		Ultramarine	$Na_6Ca_6(Al_6S_{i6}O_{24})$ $(SO_4$, S, S_2, S_3, Cl, $OH)_2$	8.69
979	(a)	Iron Gall Ink	Ferric Gallate $C_{21}H_{15}FeO_{15}$	8.69
1007	386, 415, 297, 92, 1134, 1087, 244, 496, 550, 617, 669, 145, 1297, 1434	Yellow Ochre	Iron (III) Oxide Hydrate, Fe_2O_3 H_2O +clay +silica	8.69
1037	1596br	Lamp Black	Carbon, C	0.37
1298br	1550br	Bistre	Wood soot, Carbon C	1.24
1300br	1554br	Sepia	Melanin $C_{18}H_{10}N_2O_4$	0.86
1307	1593br	Ivory Black	Calcium hydroxide phosphate, $Ca_5(OH)$ $(PO_4)_3$ + Carbon, C	0.86
1309	1589br	Carbon Black	Carbon, C	0.37
1318	1292, 1470br, 1448br	Purple Madder	Alizarin $C_{14}H_8O_4$ and Purpurin $C_{14}H_8O_5$	1.24
1321	1472, 1301br	Alizarin Purple	Alizarin $C_{14}H_8O_4$	0.12
1472	1328, 1187	Alizarin Crimson	Alizarin $C_{14}H_8O_4$	0.37
1571	252, 544, 1582, 133, 101,265, 275, 599, 1224, 1310, 235, 674, 757, 182, 635, 1364, 1460, 172, 310, 73, 1015, 1246, 1625, 1146, 870, 1702	Indigo	Indigo, $C_{16}H_{10}N_2O_2$	1.24
1593	1435, 1632, 1453sh, 1331, 370, 1221, 1247, 1281	Gamboge	Gambogic Acid, $C_{38}H_{44}O_8$	8.69

Table 6 Characteristic peaks of Raman spectra of pigments acquired with a 532 nm excitation source. (a) Range between 100-2500 cm^{-1}**.** Broad bands are labelled with "br", shoulder bands are labelled with "sh"

Black pigments and inks. Carbon black, ivory black, lamp black and bistre (Figure 25, 26, 27 and 28 respectively) are all characterized by broad bands between 1300 cm^{-1} and 1600 cm^{-1} due to the amorphous carbon. It is not possible to distinguish one from the others using a Raman spectroscopy [91]. In a previous work a band at 965 cm^{-1} is recorded for ivory black, but it is not present in these spectra. The 785nm laser seemed to be the one that provided the less intense peaks for

View Article Online
DOI: 10.1039/C8AY00016F

all these black pigments. The sepia also shows two broad bands, but they are generated by melanin, the main constituent of the pigment [92, 93]. Iron gall ink presents a peak at circa 980 cm^{-1} in the spectra collected (Figure 30) with the two NIR sources, then a broad band in between 560 and 570 cm^{-1} that can be observed in the 532 and 785 nm spectra, as well as one at about 1350 cm^{-1}. The spectrum acquired with the green laser has also peaks at 1601 cm^{-1} and 1644 cm^{-1}. Historically better spectra have been obtained for this pigment[94], however we were not able to reproduce these results at the lower power densities. Caput mortuum (Figure 4) has been already considered among the iron oxide based red pigments.

Conclusions

This work seeks to provide an updated and useful reference handbook for identification by Raman spectroscopy of medieval pigments meeting the needs of researchers working with portable equipment in situ and the increase in the availability of different wavelength lasers. Table 1 helps in choosing the best excitation wavelength to investigate expected pigments on a specific artefact. Indeed, the discussion of the spectra calls attention to the different phenomena that can occur according to the nature of the pigment and the wavelength used to investigate it, for example in considering the resonance Raman condition and how this effects relative peak intensities in comparison to normal Raman effect. The collection of spectra helps to compare the experimental data with references acquired with the same laser source, to unequivocally identify the pigment. The Tables 2-6 provide a practical guide, which in few steps allows the identification of pigments. Since the intensities of peaks vary according to the exciting source, the operator can search references recorded with the same wavelength used during the measurements. New pigment references collected with wavelengths not used in previous works are also provided. This work also concludes that it is evident that the Raman technique alone is not capable of fully characterizing all the pigments selected, especially the fluorescent organic dyes that are presenting challenges to curators. This highlights the need to turn to other techniques that can provide complementary information.

Acknowledgements

The authors would like to thank the Northumbria University, Durham University and Rutherford Appleton Laboratory, Harwell Campus, Didcot. G. Marucci is also thankful to C. Aibéo, Rathgenforschungslabor (Berlin), for her advice. Funding for this project was provided through EPSRC DTA studentship at Northumbria University, STFC for instrument time at Harwell, and kind donations from Rob and Felicity Shepherd.

Notes and references

1. L. Burgio, R. J. H. Clark and S. Firth, *Analyst*, 2001, **126**, 222-227.
2. M. Aceto, A. Agostino, G. Fenoglio, M. Gulmini, V. Bianco and E. Pellizzi, *Spectrochimica Acta Part a-Molecular and Biomolecular Spectroscopy*, 2012, **91**, 352-359.
3. J. Aramendia, L. Gomez‐Nubla, K. Castro, I. Martinez‐Arkarazo, D. Vega, A. Sanz López de Heredia, A. García Ibáñez de Opakua and J. Madariaga, *Journal of Raman Spectroscopy*, 2012, **43**, 1111-1117.
4. C. Boschetti, A. Corradi and P. Baraldi, *Journal of Raman Spectroscopy*, 2008, **39**, 1085-1090.
5. P. Colomban, *Journal of Cultural Heritage*, 2008, **9**, E55-E60.
6. P. Colomban, *Journal of Raman Spectroscopy*, 2012, **43**, 1529-1535.
7. P. Colomban, V. Milande and L. Le Bihan, *Journal of Raman Spectroscopy*, 2004, **35**, 527-535.
8. P. Colomban, V. Milande and H. Lucas, *Journal of Raman Spectroscopy*, 2004, **35**, 68-72.
9. P. Colomban and A. Tournie, *Journal of Cultural Heritage*, 2007, **8**, 242-256.
10. P. Colomban, A. Tournie, M. C. Caggiani and C. Paris, *Journal of Raman Spectroscopy*, 2012, **43**, 1975-1984.
11. C. Colombo, F. Bevilacqua, L. Brambilla, C. Conti, M. Realini, J. Striova and G. Zerbi, *Analytical and Bioanalytical Chemistry*, 2011, **401**, 757-765.
12. D. de Waal, *Journal of Raman Spectroscopy*, 2009, **40**, 2162-2170.
13. M. K. Donais, D. George, B. Duncan, S. M. Wojtas and A. M. Daigle, *Analytical Methods*, 2011, **3**, 1061-1071.
14. D. Hutsebaut, P. Vandenabeele and L. Moens, *Analyst*, 2005, **130**, 1204-1214.
15. B. Kirmizi, P. Colomban and M. Blanc, *Journal of Raman Spectroscopy*, 2010, **41**, 1240-1247.
16. B. Kirmizi, P. Colomban and B. Quette, *Journal of Raman Spectroscopy*, 2010, **41**, 780-790.
17. D. Lauwers, A. G. Hutado, V. Tanevska, L. Moens, D. Bersani and P. Vandenabeele, *Spectrochimica Acta Part a-Molecular and Biomolecular Spectroscopy*, 2014, **118**, 294-301.
18. D. Mancini, A. Tournie, M. C. Caggiani and P. Colomban, *Journal of Raman Spectroscopy*, 2012, **43**, 294-302.
19. M. Pérez-Alonso, K. Castro, I. Martinez-Arkarazo, M. Angulo, M. Olazabal and J. Madariaga, *Analytical and bioanalytical chemistry*, 2004, **379**, 42-50.
20. I. Reiche and L. Lambacher, *Journal of Raman Spectroscopy*, 2004, **35**, 719-725.
21. P. Ricciardi, P. Colomban, A. Tournie, M. Macchiarola and N. Ayed, *Journal of Archaeological Science*, 2009, **36**, 2551-2559.
22. P. Ropret and J. M. Madariaga, *Journal of Raman Spectroscopy*, 2014, **45**, 985-992.
23. F. Rosi, V. Manuali, T. Grygar, P. Bezdicka, B. G. Brunetti, A. Sgamellotti, L. Burgio, C. Seccaronif and C. Miliani, *Journal of Raman Spectroscopy*, 2011, **42**, 407-414.
24. D. C. Smith, *Spectrochimica Acta Part a-Molecular and Biomolecular Spectroscopy*, 2003, **59**, 2353-2369.
25. A. Tournie, L. C. Prinsloo, C. Paris, P. Colomban and B. Smith, *Journal of Raman Spectroscopy*, 2011, **42**, 399-406.

View Article Online
DOI: 10.1039/C8AY00016F

26. P. Vandenabeele, K. Castro, M. Hargreaves, L. Moens, J. M. Madariaga and H. G. M. Edwards, *Analytica Chimica Acta*, 2007, **588**, 108-116.
27. P. Vandenabeele, H. G. M. Edwards and J. Jehlicka, *Chemical Society Reviews*, 2014, **43**, 2628-2649.
28. P. Vandenabeele, F. Verpoort and L. Moens, *Journal of Raman Spectroscopy*, 2001, **32**, 263-269.
29. P. Vandenabeele, T. L. Weis, E. R. Grant and L. J. Moens, *Analytical and Bioanalytical Chemistry*, 2004, **379**, 137-142.
30. M. A. Ziemann, *Journal of Raman Spectroscopy*, 2006, **37**, 1019-1025.
31. D. Bersani, C. Conti, P. Matousek, F. Pozzi and P. Vandenabeele, *Analytical Methods*, 2016, **8**, 8395-8409.
32. R. J. H. Clark, *Chemical Society Reviews*, 1995, **24**, 187-196.
33. L. M. Proniewicz, C. Paluszkiewicz, A. Wesełucha-Birczyńska, H. Majcherczyk, A. Barański and A. Konieczna, *Journal of Molecular Structure*, 2001, **596**, 163-169.
34. P. Vandenabeele, B. Wehling, L. Moens, H. Edwards, M. De Reu and G. Van Hooydonk, *Analytica Chimica Acta*, 2000, **407**, 261-274.
35. T. D. Chaplin, R. J. Clark, D. Jacobs, K. Jensen and G. D. Smith, *Analytical chemistry*, 2005, **77**, 3611-3622.
36. A. S. Lee, P. J. Mahon and D. C. Creagh, *Vibrational Spectroscopy*, 2006, **41**, 170-175.
37. I. M. Bell, R. J. H. Clark and P. J. Gibbs, *Spectrochimica Acta Part a-Molecular and Biomolecular Spectroscopy*, 1997, **53**, 2159-2179.
38. M. Bouchard and D. C. Smith, *Spectrochimica Acta Part a-Molecular and Biomolecular Spectroscopy*, 2003, **59**, 2247-2266.
39. L. Burgio and R. J. H. Clark, *Spectrochimica Acta Part a-Molecular and Biomolecular Spectroscopy*, 2001, **57**, 1491-1521.
40. M. Aceto, A. Agostino, G. Fenoglio, P. Baraldi, P. Zannini, C. Hofmann and E. Gamillscheg, *Spectrochimica Acta Part a-Molecular and Biomolecular Spectroscopy*, 2012, **95**, 235-245.
41. D. Bersani, P. P. Lottici, F. Vignalil and G. Zanichelli, *Journal of Raman Spectroscopy*, 2006, **37**, 1012-1018.
42. S. P. Best, R. J. H. Clark, M. A. M. Daniels, C. A. Porter and R. Withnall, *Studies in Conservation*, 1995, **40**, 31-40.
43. S. Bioletti, R. Leahy, J. Fields, B. Meehan and W. Blau, *Journal of Raman Spectroscopy*, 2009, **40**, 1043-1049.
44. K. L. Brown and R. J. H. Clark, *Journal of Raman Spectroscopy*, 2004, **35**, 4-12.
45. K. L. Brown and R. J. H. Clark, *Journal of Raman Spectroscopy*, 2004, **35**, 181-189.
46. K. L. Brown and R. J. H. Clark, *Journal of Raman Spectroscopy*, 2004, **35**, 217-223.
47. S. Bruni, S. Caglio, V. Guglielmi and G. Poldi, *Applied Physics a-Materials Science & Processing*, 2008, **92**, 103-108.
48. L. Burgio, D. A. Ciomartan and R. J. H. Clark, *Journal of Raman Spectroscopy*, 1997, **28**, 79-&.
49. G. Chapman, *Manuscripta*, 1986, **30**, 168-169.
50. R. J. Clark, *Chemical Society Reviews*, 1995, **24**, 187-196.
51. R. J. H. Clark and P. J. Gibbs, *Journal of Archaeological Science*, 1998, **25**, 621-629.
52. R. J. H. Clark and J. van der Weerd, *Journal of Raman Spectroscopy*, 2004, **35**, 279-+.
53. M. Clarke, *Studies in Conservation*, 2004, **49**, 231-244.
54. A. Deneckere, M. De Reu, M. P. J. Martens, K. De Coene, B. Vekemans, L. Vincze, P. De Maeyer, P. Vandenabeele and L. Moens, *Spectrochimica Acta Part a-Molecular and Biomolecular Spectroscopy*, 2011, **80**, 125-132.
55. B. Doherty, A. Daveri, C. Clementi, A. Romani, S. Bioletti, B. Brunetti, A. Sgamellotti and C. Miliani, *Spectrochimica Acta Part a-Molecular and Biomolecular Spectroscopy*, 2013, **115**, 330-336.
56. A. Duran, A. Lopez-Montes, J. Castaing and T. Espejo, *Journal of Archaeological Science*, 2014, **45**, 52-58.
57. H. G. M. Edwards, D. W. Farwell, F. R. Perez and J. M. Garcia, *Analyst*, 2001, **126**, 383-388.
58. D. Lauwers, V. Cattersel, L. Vandamme, A. Van Eester, K. De Langhe, L. Moens and P. Vandenabeele, *Journal of Raman Spectroscopy*, 2014, **45**, 1266-1271.
59. A. Le Gac, S. Pessanha, S. Longelin, M. Guerra, J. C. Frade, F. Lourenco, M. C. Serrano, M. Manso and M. L. Carvalho, *Applied Radiation and Isotopes*, 2013, **82**, 242-257.
60. K. Nesmerak and I. Nemcova, *Analytical Letters*, 2012, **45**, 330-344.
61. K. Trentelman and N. Turner, *Journal of Raman Spectroscopy*, 2009, **40**, 577-584.
62. G. Van Der Snickt, W. De Nolf, B. Vekemans and K. Janssens, *Applied Physics a-Materials Science & Processing*, 2008, **92**, 59-68.
63. G. Van Hooydonk, M. De Reu, L. Moens, J. Van Aelst and L. Milis, *European Journal of Inorganic Chemistry*, 1998, 639-644.
64. P. Vandenabeele, B. Wehling, L. Moens, B. Dekeyzer, B. Cardon, A. von Bohlen and R. Klockenkamper, *Analyst*, 1999, **124**, 169-172.
65. B. Wehling, P. Vandenabeele, L. Moens, R. Klockenkamper, A. von Bohlen, G. Van Hooydonk and M. de Reu, *Mikrochimica Acta*, 1999, **130**, 253-260.
66. A. Zoleo, L. Nodari, M. Rampazzo, F. Piccinelli, U. Russo, C. Federici and M. Brustolon, *Archaeometry*, 2014, **56**, 496-512.
67. C. Cennini, *Il libro dell'arte, a cura di Fabio Frezzato*, Neri Pozza, Vicenza, 3rd Edition edn., 2006.
68. M. Fryling, C. J. Frank and R. L. McCreery, *Applied spectroscopy*, 1993, **47**, 1965-1974.
69. K. J. Frost and R. L. Mccreery, *Applied spectroscopy*, 1998, **52**, 1614-1618.
70. P. Vandenabeele and L. Moens, *Journal of Raman Spectroscopy*, 2012, **43**, 1545-1550.
71. R. L. McCreery, *Raman Spectroscopy for Chemical Analysis*, United States of America, 10 edn., 2000.
72. P. Vandenabeele, *Practical Raman Spectroscopy: an introduction*, First edition edn., 2013.
73. J. D. Ingle Jr and S. R. Crouch, 1988, 141-142.
74. presented in part at the Workshop on Preparation of Historical Lake Pigments 23-25 March 2011

Doerner Institut, Bayerische Staatsgemaeldesammlungen, Muenchen (Germany), 2011.

75. *The Non-Destructive and in-situ identification of controlled drugs and narcotics*, Horiba Scientific, France.
76. A. Coccato, D. Bersani, A. Coudray, J. Sanyova, L. Moens and P. Vandenabeele, *Journal of Raman Spectroscopy*, 2016, DOI: 10.1002/jrs.4956, n/a-n/a.

View Article Online
DOI: 10.1039/C8AY00016F

77. M. Caggiani, A. Cosentino and A. Mangone, *Microchemical Journal*, 2016, **129**, 123-132.
78. D. Bikiaris, S. Daniilia, S. Sotiropoulou, O. Katsimbiri, E. Pavlidou, A. Moutsatsou and Y. Chryssoulakis, *Spectrochimica Acta Part A: Molecular and Biomolecular Spectroscopy*, 2000, **56**, 3-18.
79. D. Lau, C. Villis, S. Furman and M. Livett, *Analytica chimica acta*, 2008, **610**, 15-24.
80. M. Leona, *Proc Natl Acad Sci*, 2009, **106**.
81. A. V. Whitney, R. P. Van Duyne and F. Casadio, *Journal of Raman Spectroscopy*, 2006, **37**, 993-1002.
82. F. Pozzi, J. R. Lombardi and M. Leona, *Heritage Science*, 2013, **1**, 1-8.
83. *Journal*.
84. A. Coccato, D. Bersani, A. Coudray, J. Sanyova, L. Moens and P. Vandenabeele, *Journal of Raman Spectroscopy*, 2016.
85. A. Cosentino, *e-conservation Journal*, 2014, **2**, 57-68.
86. E. Mattei, G. De Vivo, A. De Santis, C. Gaetani, C. Pelosi and U. Santamaria, *Journal of Raman Spectroscopy*, 2008, **39**, 302-306.
87. R. Clark and M. Franks, *Chemical Physics Letters*, 1975, **34**, 69-72.
88. P. Pouli, D. C. Emmony, C. E. Madden and I. Sutherland, *Journal of Cultural Heritage*, 2003, **4**, 271-275.
89. C. Goodeve, *Transactions of the Faraday Society*, 1937, **33**, 340-347.
90. M. Leona, J. Stenger and E. Ferloni, *Journal of Raman Spectroscopy*, 2006, **37**.
91. E. P. Tomasini, E. B. Halac, M. Reinoso, E. J. Di Liscia and M. S. Maier, *Journal of Raman Spectroscopy*, 2012, **43**, 1671-1675.
92. S. A. Centeno and J. Shamir, *Journal of Molecular Structure*, 2008, **873**, 149-159.
93. Z. Huang, H. Lui, X. Chen, A. Alajlan, D. I. McLean and H. Zeng, *Journal of biomedical optics*, 2004, **9**, 1198-1205.
94. M. Bicchieri, M. Monti, G. Piantanida and A. Sodo, *All that is iron - ink is not always iron - gall!*, 2008.

View Article Online
DOI: 10.1039/C8AY00016F

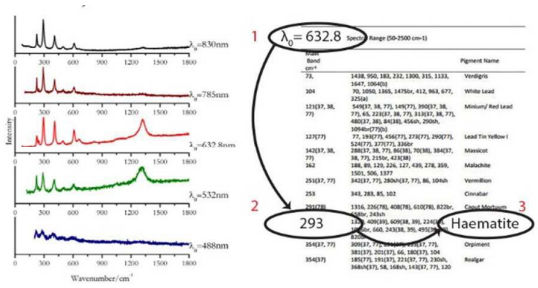

Stepwise identification of medieval pigments by Raman spectra data and excitation source.

View Article Online
DOI: 10.1039/C8AY00016F

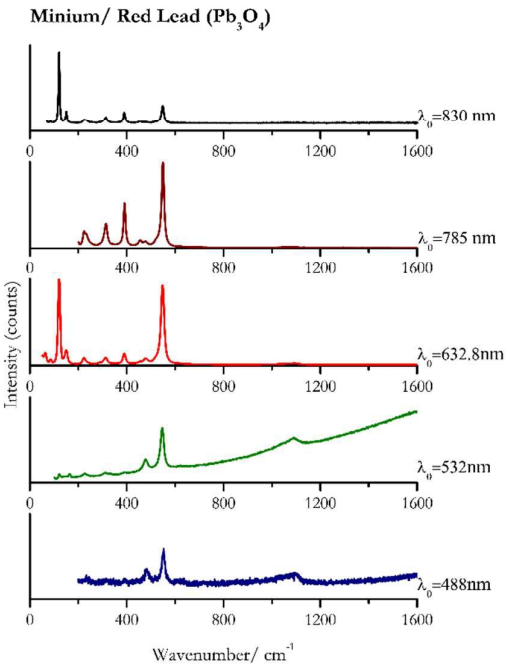

Figure 1 Raman spectra of Minium or Red Lead

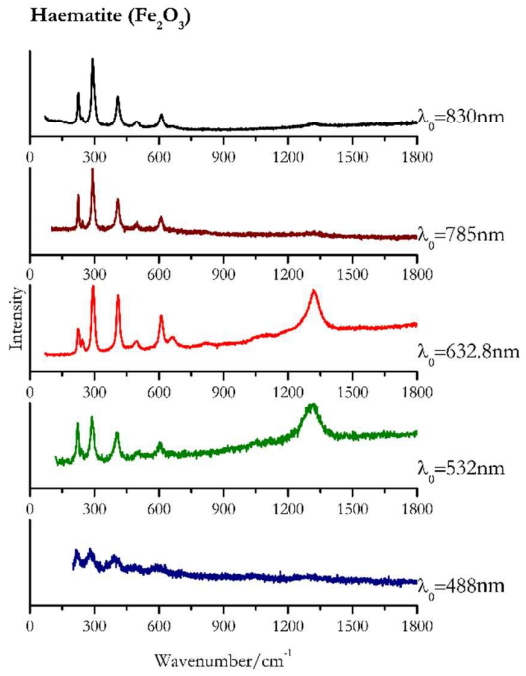

Figure 2 Raman spectra of Haematite

View Article Online
DOI: 10.1039/C8AY00016F

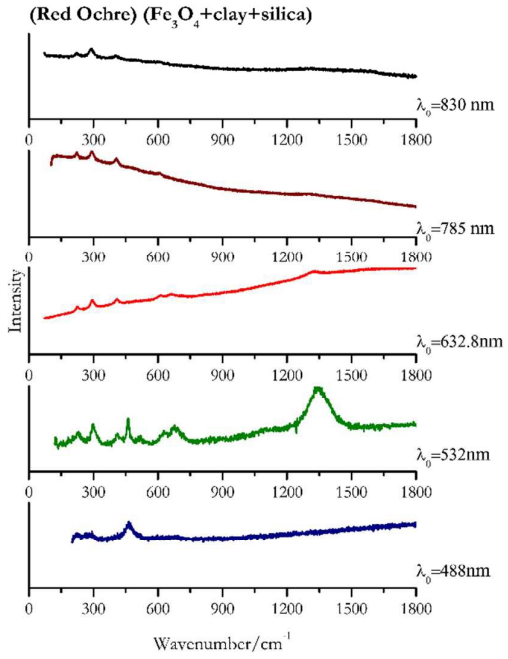

Figure 3 Raman spectra of Red Ochre

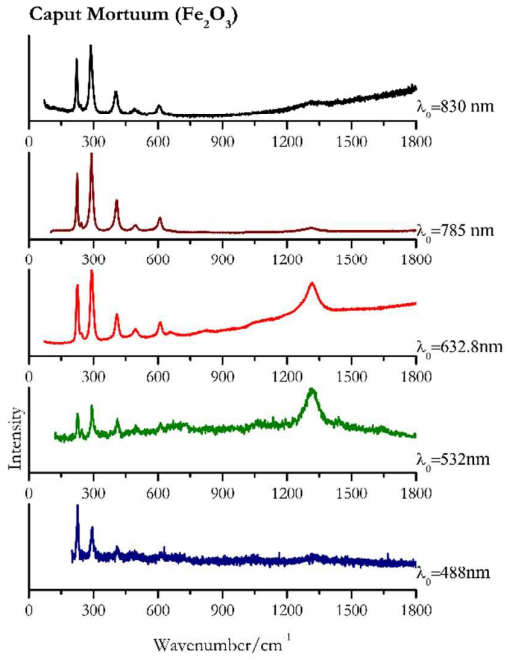

Figure 4 Raman spectra of Caput Mortuum

View Article Online
DOI: 10.1039/C8AY00016F

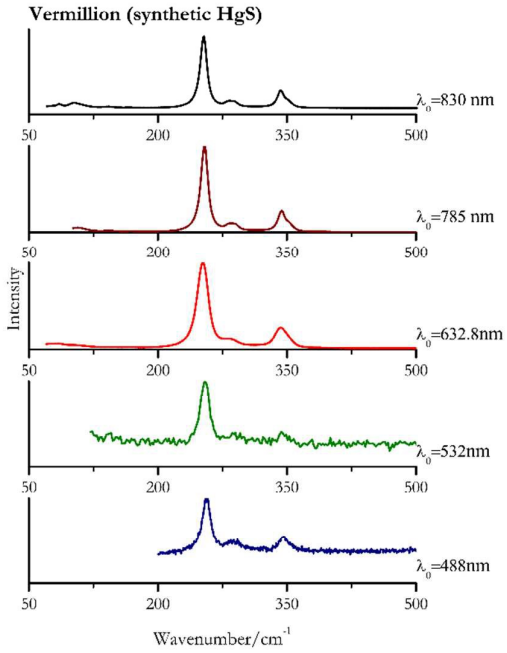

Figure 5 Raman spectra of Vermillion

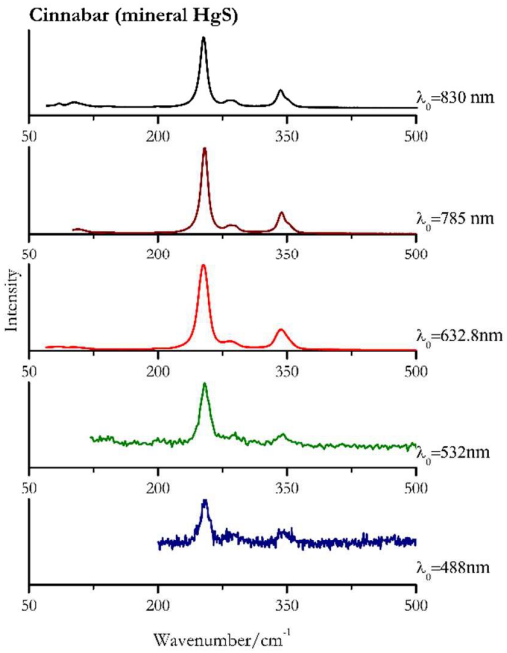

Figure 6 Raman spectra of Cinnabar

View Article Online
DOI: 10.1039/C8AY00016F

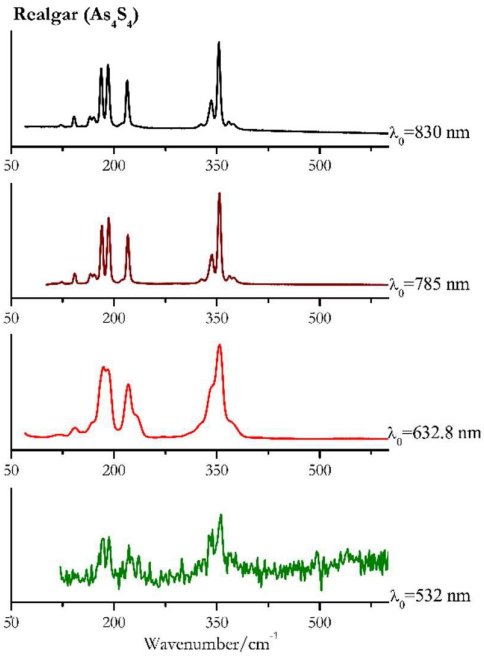

Figure 7 Raman spectra of Realgar

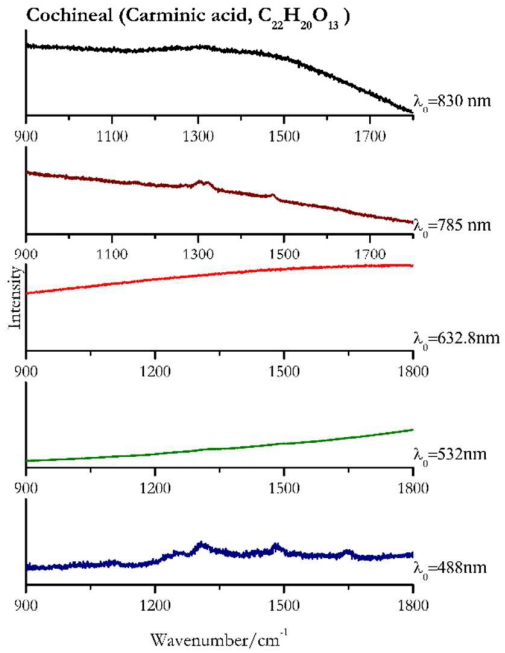

Figure 8 Raman spectra of Cochineal

View Article Online
DOI: 10.1039/C8AY00016F

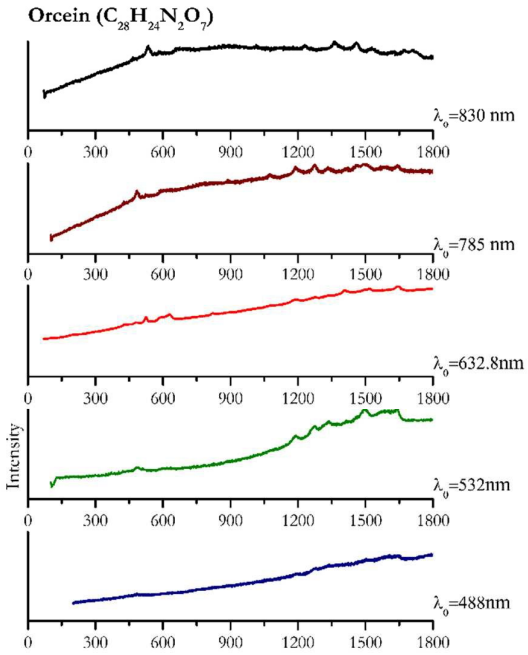

Figure 9 Raman spectra of Orcein

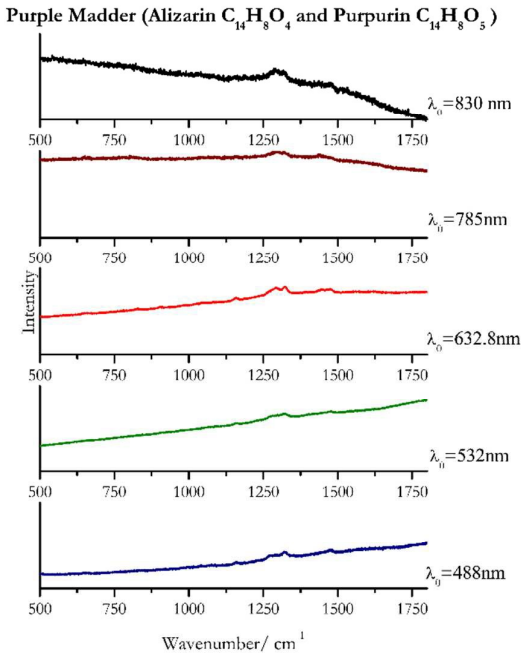

Figure 10 Raman spectra of Purple Madder

View Article Online
DOI: 10.1039/C8AY00016F

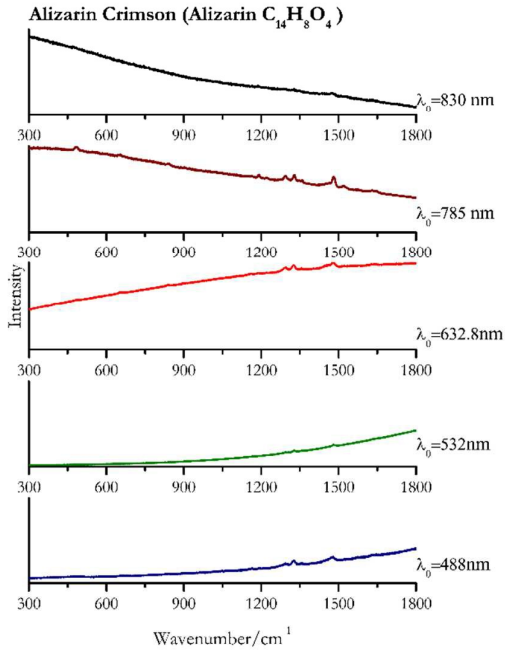

Figure 11 Raman spectra of Alizarin Crimson

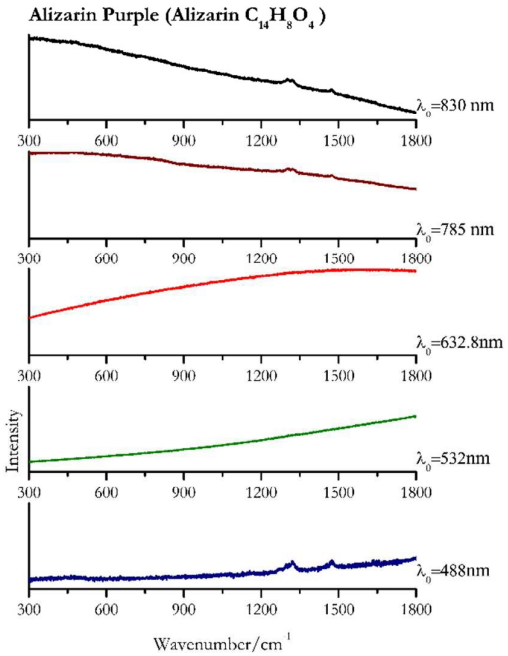

Figure 12 Raman spectra of Alizarin Purple

View Article Online
DOI: 10.1039/C8AY00016F

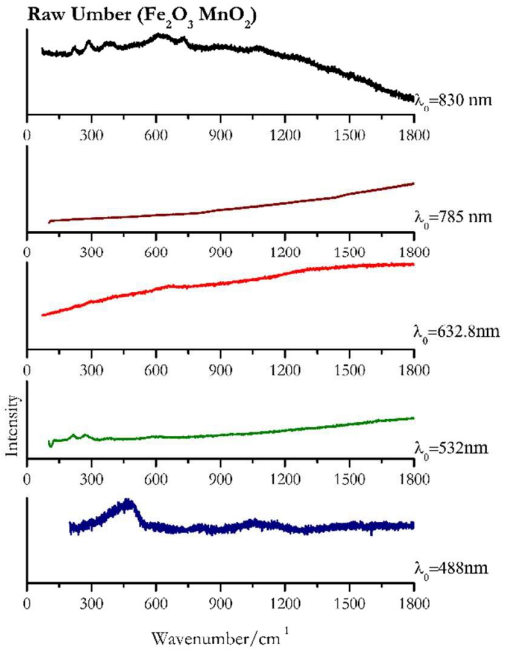

Figure 13 Raman spectra of Raw Umber

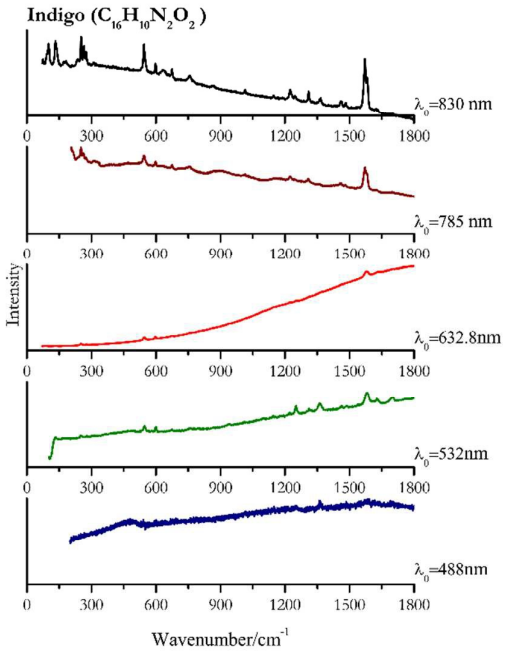

Figure 14 Raman spectra of Indigo

View Article Online
DOI: 10.1039/C8AY00016F

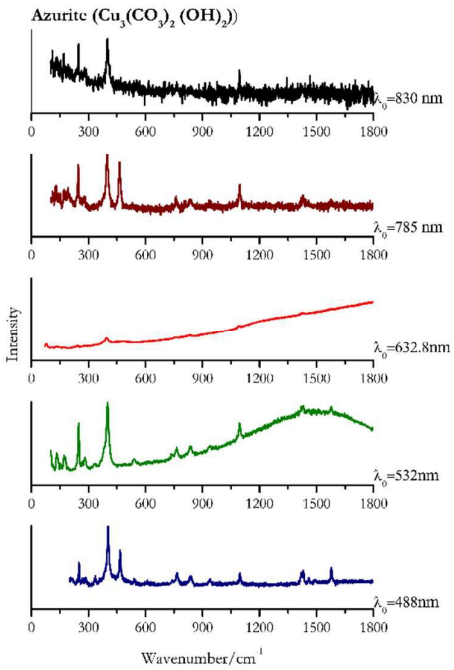

Figure 15 Raman spectra of Azurite

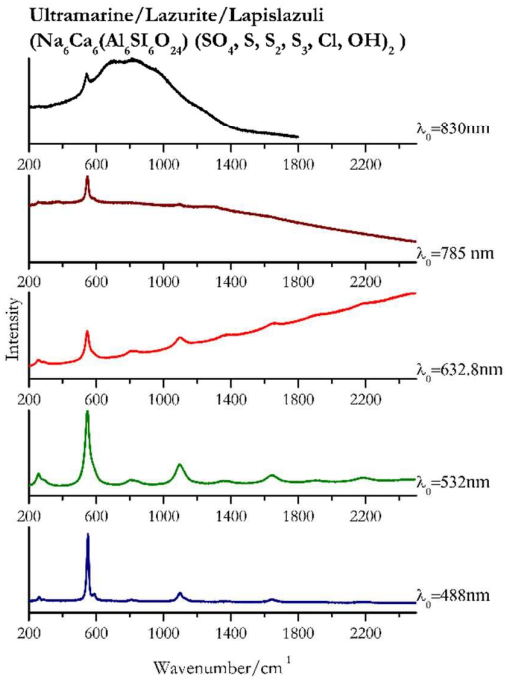

Figure 16 Raman spectra of Ultramarine

View Article Online
DOI: 10.1039/C8AY00016F

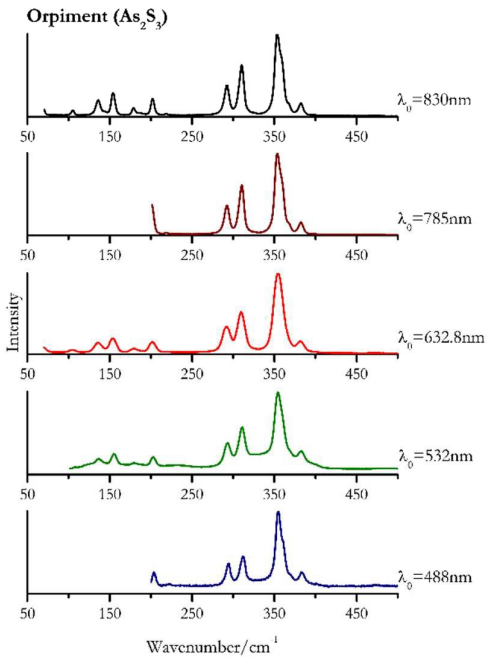

Figure 17 Raman spectra of Orpiment

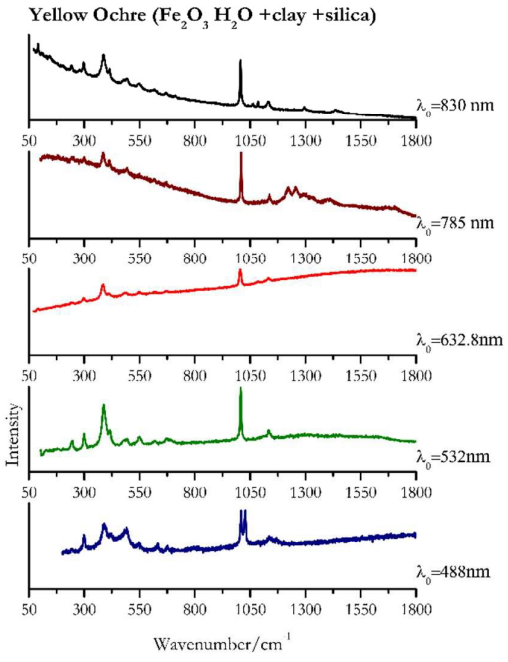

Figure 18 Raman spectra of Yellow Ochre

View Article Online
DOI: 10.1039/C8AY00016F

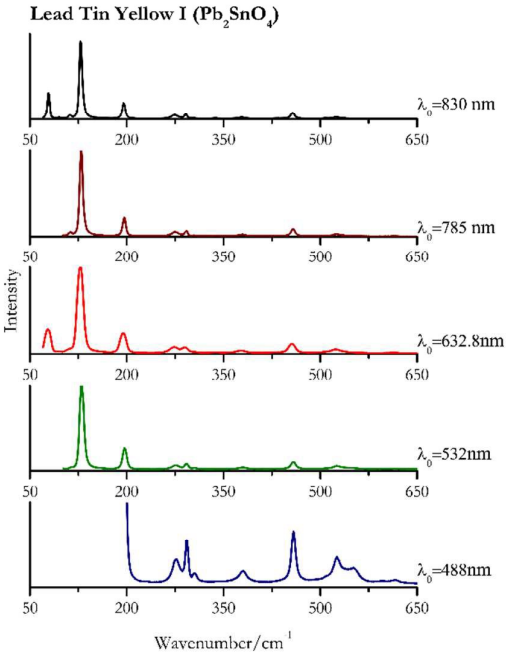

Figure 19 Raman spectra of Lead Tin Yellow I

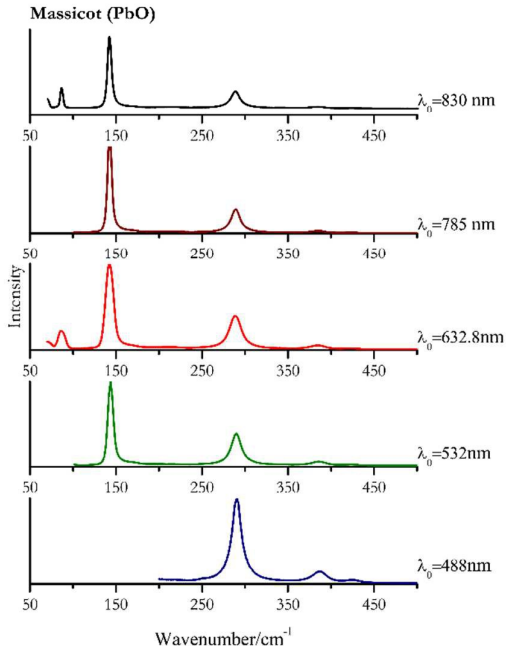

Figure 20 Raman spectra of Massicot

View Article Online
DOI: 10.1039/C8AY00016F

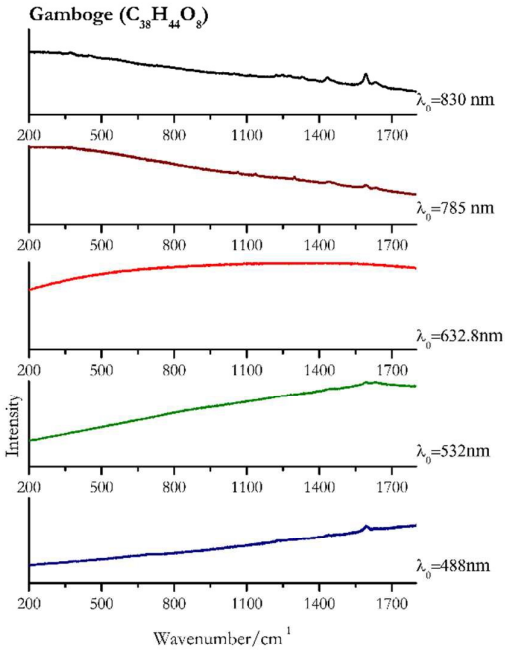

Figure 21 Raman spectra of Gamboge

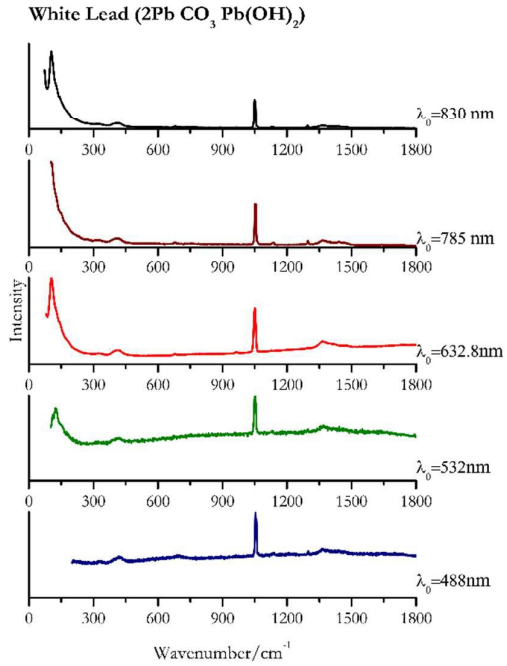

Figure 22 Raman spectra of White Lead

View Article Online
DOI: 10.1039/C8AY00016F

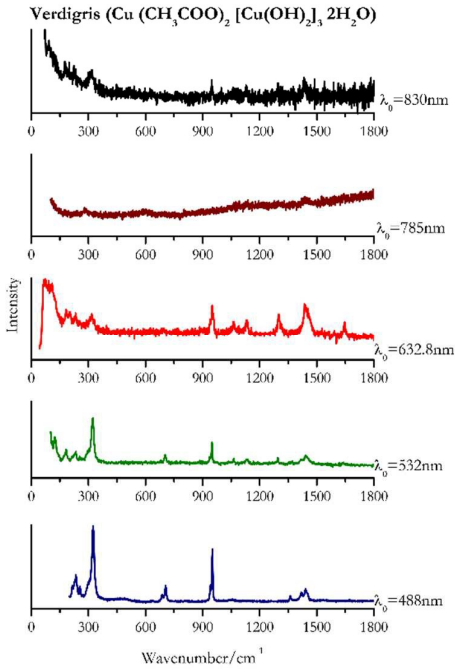

Figure 23 Raman spectra of Verdigris.

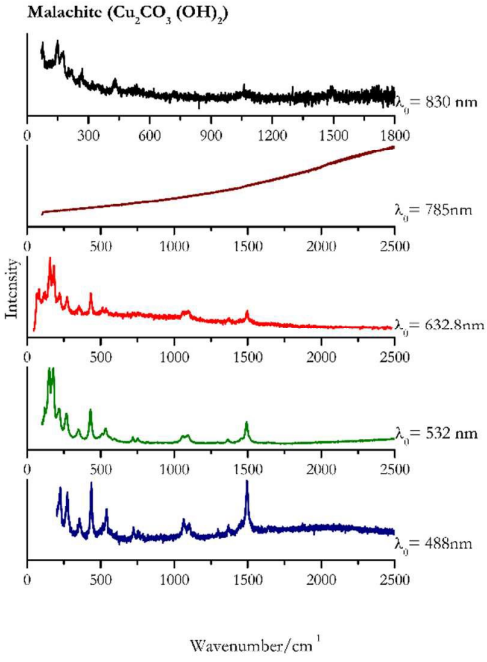

Figure 24 Raman spectra of Malachite

View Article Online
DOI: 10.1039/C8AY00016F

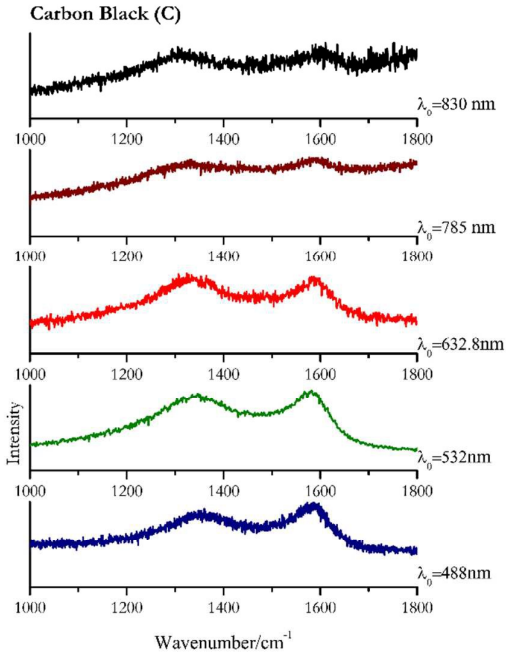

Figure 25 Raman spectra of Carbon Black

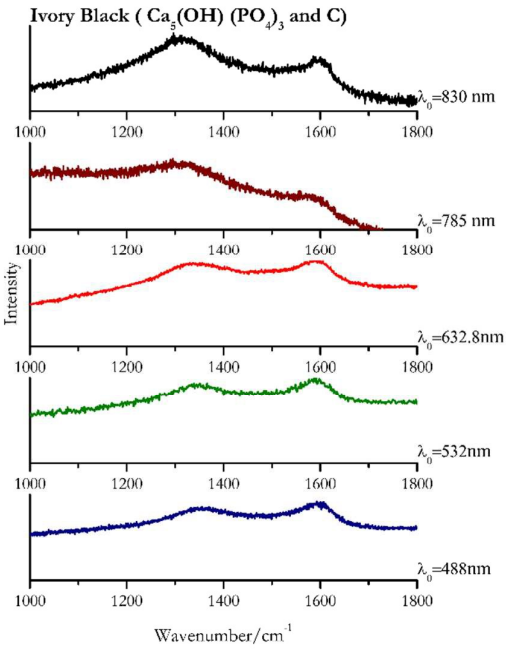

Figure 26 Raman spectra of Ivory Black

View Article Online
DOI: 10.1039/C8AY00016F

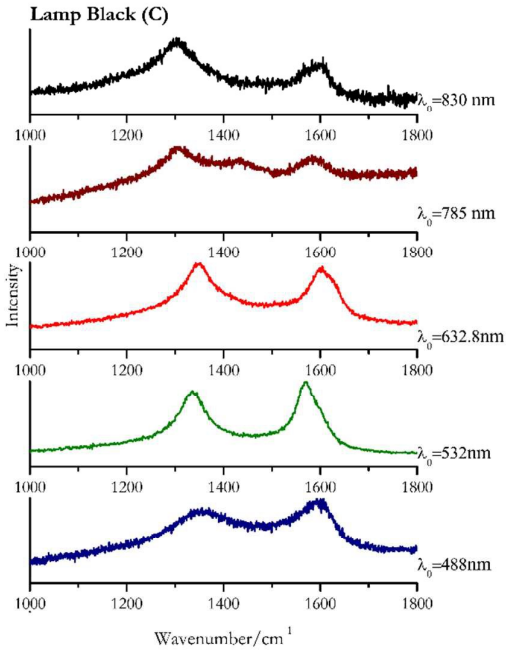

Figure 27 Raman spectra of Lamp Black

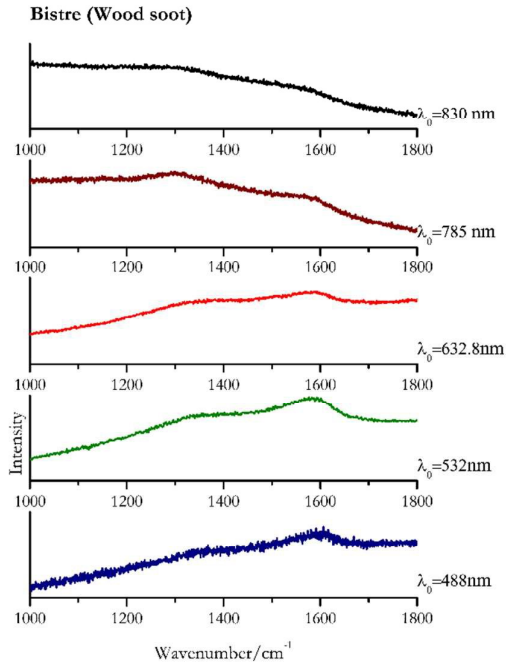

Figure 28 Raman spectra of Bistre

View Article Online
DOI: 10.1039/C8AY00016F

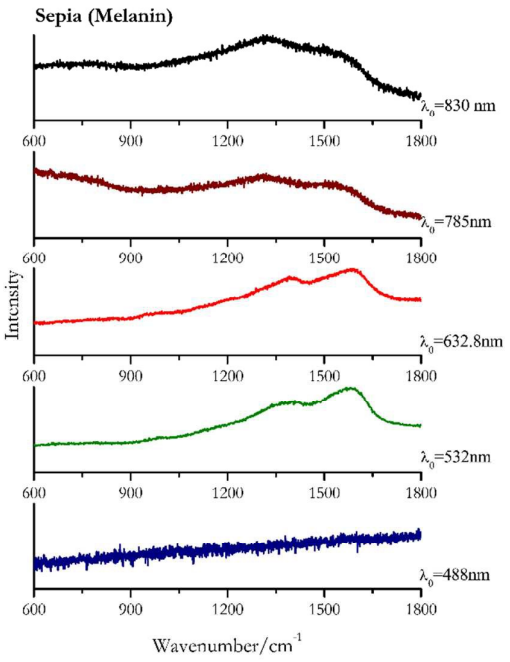

Figure 29 Raman spectra of Sepia

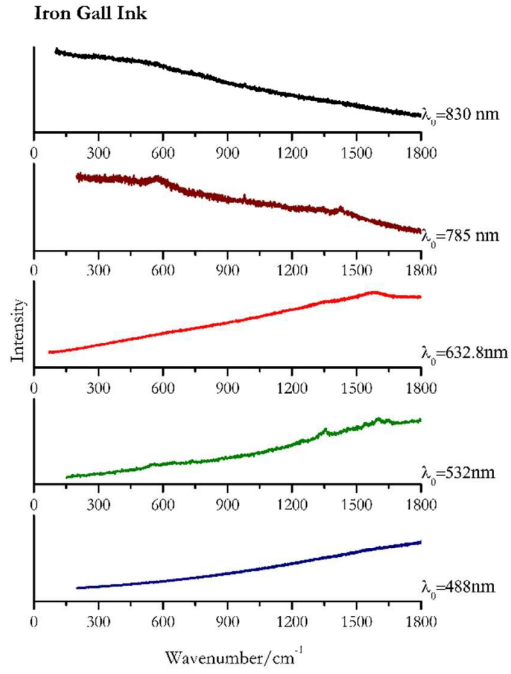

Figure 30 Raman spectra of Iron Gall Ink